

OPEN

# CO<sub>2</sub> oxidative coupling of methane using an earth-abundant CaO-based catalyst

Yongzheng Zhang<sup>1,4</sup>, Yohei Cho<sup>2</sup>, Akira Yamaguchi<sup>2</sup>, Xiaobo Peng<sup>3</sup>, Masahiro Miyauchi<sup>2</sup>, Hideki Abe<sup>3</sup> & Takeshi Fujita<sup>1\*</sup>

CO<sub>2</sub> oxidative coupling of methane has been achieved by using CO<sub>2</sub> as the oxidant. We explored various catalysts with the capability of producing C<sub>2,3</sub> hydrocarbons and found that the use of a CaO-based oxide with sodium (Na) and chloride (Cl) allowed for remarkable direct methane conversion with a C<sub>2,3</sub> yield of 6.6% at 950 °C. Microstructural characterisations showed that the optimal sample contained sodium carbonate (Na<sub>2</sub>CO<sub>3</sub>) covered with fine calcium oxide particles with chloride doping. Interestingly, sodium carbonate acted as a molten salt catalyst in this scenario. The synthesised active components are earth-abundant and can increase the possibility of achieving higher yields of hydrocarbons.

Effective utilisation of methane (CH<sub>4</sub>) and carbon dioxide (CO<sub>2</sub>) is important for realising a more sustainable society because these are the major components of natural and greenhouse gases. Catalytic reforming of CH<sub>4</sub> with CO<sub>2</sub> is known as dry reforming of methane (DRM) to syngas (H<sub>2</sub> + CO): CH<sub>4</sub> + CO<sub>2</sub> → 2CO + 2 H<sub>2</sub><sup>1,2</sup>. However, other possible reaction pathways to synthesise C<sub>2</sub> or higher hydrocarbons are also possible, in which CO<sub>2</sub> is used as an oxidant: 2CH<sub>4</sub> + 2CO<sub>2</sub> → C<sub>2</sub>H<sub>4</sub> + 2CO + 2H<sub>2</sub>O and 2CH<sub>4</sub> + CO<sub>2</sub> → C<sub>2</sub>H<sub>6</sub> + CO + H<sub>2</sub>O<sup>3,4</sup>. Although oxidative coupling of methane (OCM) using O<sub>2</sub> as an oxidant has been known as a useful reaction to directly convert methane to C<sub>2</sub> or higher hydrocarbons since the 1980s<sup>5–8</sup>, corresponding reactions using CO<sub>2</sub> in CO<sub>2</sub>-OCM are quite challenging to achieve. So far, explorative studies investigating many oxides and their mixtures have been reported<sup>3,9</sup>, which attained C<sub>2</sub> yields of 3–4% using modified CeO<sub>2</sub> with CaO as the effective catalyst<sup>10,11</sup>, but the corresponding yields are still insufficient.

Based on previous knowledge and our explorative search for various catalysts, we found that mixed Ca- and Na-based oxides, synthesised via a chemical route with additive NaCl, show direct methane conversion with a remarkable C<sub>2,3</sub> yield of ~6% at 950 °C. The polymerised complex (PC) method is the most studied and frequently used technique for the preparation of oxides because these methods can accurately control the final composition and yield pure and homogeneous oxides<sup>12,13</sup>. It was thus used in this study to ensure optimal results and reproducibility of experiments. Microstructural characterisation indicated that the product was uniform Na<sub>2</sub>CO<sub>3</sub> covered with fine CaO particles with Cl doping. Interestingly, the Na<sub>2</sub>CO<sub>3</sub> works as a molten salt catalyst at the reaction temperature of interest. The complex CaO-based oxides produced in this study are inexpensive and earth-abundant in the sea and would widen the opportunity to attain higher yields of hydrocarbons via CO<sub>2</sub>-OCM.

## Results and Discussion

The first key finding was that the addition of Na to modified CaO oxides in the PC method was effective for hydrocarbon generation. Figure 1(a) shows the dependence of the C<sub>2,3</sub> yield on the molar ratio of Na to Ca used. When the ratio was 0.5, i.e., equal moles of Ca and Na were used, the highest C<sub>2,3</sub> yield of ~5% was obtained. For comparison, the corresponding data for commercial CaO nanopowder (Sigma-Aldrich, 98%, Product ID: 634182) with a large surface area and conventional CaO powder (Wako, 99.9%, 036-13572) are also shown, and the results indicate that the use of only CaO cannot give the high C<sub>2,3</sub> yield.

The Cl element is a well-known promoter of CH<sub>3</sub> radicals<sup>14</sup>. Therefore, in order to attain higher C<sub>2,3</sub> yields, we tested various chlorides as additives under the conditions that gave the highest C<sub>2,3</sub> yield in Fig. 1(a). As the

<sup>1</sup>School of Environmental Science and Engineering, Kochi University of Technology, 185 Miyanokuchi, Tosayamada, Kami City, Kochi, 782-8502, Japan. <sup>2</sup>Tokyo Institute of Technology, 2-12-1 Ookayama, Meguro-ku, Tokyo, 152-8552, Japan. <sup>3</sup>National Institute for Materials Science, 1-1 Namiki, Tsukuba, Ibaraki, 305-0044, Japan. <sup>4</sup>School of Physics and Physical Engineering, Qufu Normal University, Qufu, 273165, China. \*email: [fujita.takeshi@kochi-tech.ac.jp](mailto:fujita.takeshi@kochi-tech.ac.jp)

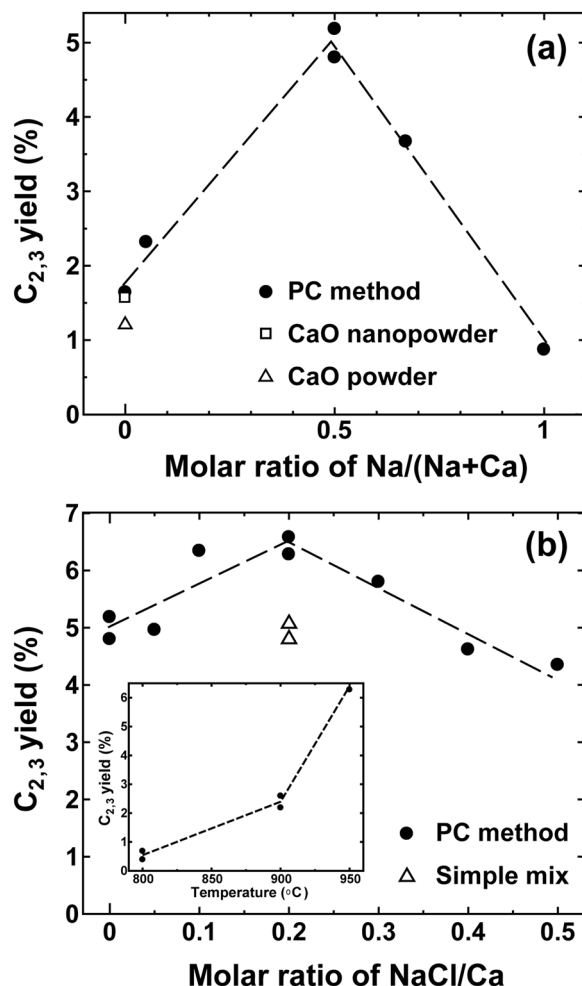


**Figure 1.** Catalytic performance at 950 °C. (a) C<sub>2,3</sub> yield against the molar ratio of Na/Ca + Na in the chemical fabrication process. (b) C<sub>2,3</sub> yield against the molar ratio of NaCl/Ca in the chemical fabrication process. The temperature dependence of the C<sub>2,3</sub> yield is also shown in the inset of (b). Measurements were performed 20 min after reaching each temperature.

Catalyst	CH <sub>4</sub> conversion (%)	C <sub>2,3</sub> yield (%)	Selectivity (%)				
			C <sub>2</sub> H <sub>2</sub>	C <sub>2</sub> H <sub>4</sub>	C <sub>2</sub> H <sub>6</sub>	C <sub>3</sub> H <sub>6</sub>	C <sub>3</sub> H <sub>8</sub>
Ca:Na:NaCl (1:1:0.2) <sup>a</sup> at 950 °C	18.9	6.6	9.2	63.3	21.5	3.4	2.6
Ca:Na:NaCl (1:1:0.2) <sup>a</sup> at 900 °C	23.1	2.5	0.9	42.6	55.6	0.9	0
CaO nanopowder at 950 °C	9.3	1.6	4.7	64	31.3	0	0

**Table 1.** Representative performance of the optimal sample and commercial CaO nanopowder. Measurements were carried out 20 min after reaching each temperature. <sup>a</sup>Optimal molar ratio of the mixture in the polymerised complex method.

second key finding, we found that the addition of NaCl was also effective in improving the yield. Figure 1(b) shows the dependence of the yield on the molar ratio of NaCl to Ca: a 20% molar ratio of NaCl to Ca gave a ~6% yield. In the ternary phase diagram for the CaCO<sub>3</sub>-Na<sub>2</sub>CO<sub>3</sub>-NaCl system<sup>15,16</sup>, the addition of NaCl lowers the melting temperature (~690 °C) effectively around the optimal composition and successful doping of Cl, and more homogeneous dispersions of composites may be realised in the synthesis process close to this composition. We summarise the representative results for the catalytic performance in Table 1. The temperature dependence of the C<sub>2,3</sub> yield is also shown in the inset of Fig. 1(b), according to which 950 °C was the optimum reaction temperature, which was instrumentally the upper limit in our experimental setup. For comparison, we also synthesised the catalysts at the optimal composition via a simple mixing procedure, but the performance (~5%) was lower than that attained by the PC method. Therefore, we considered mixing by the PC method as the optimal technique and

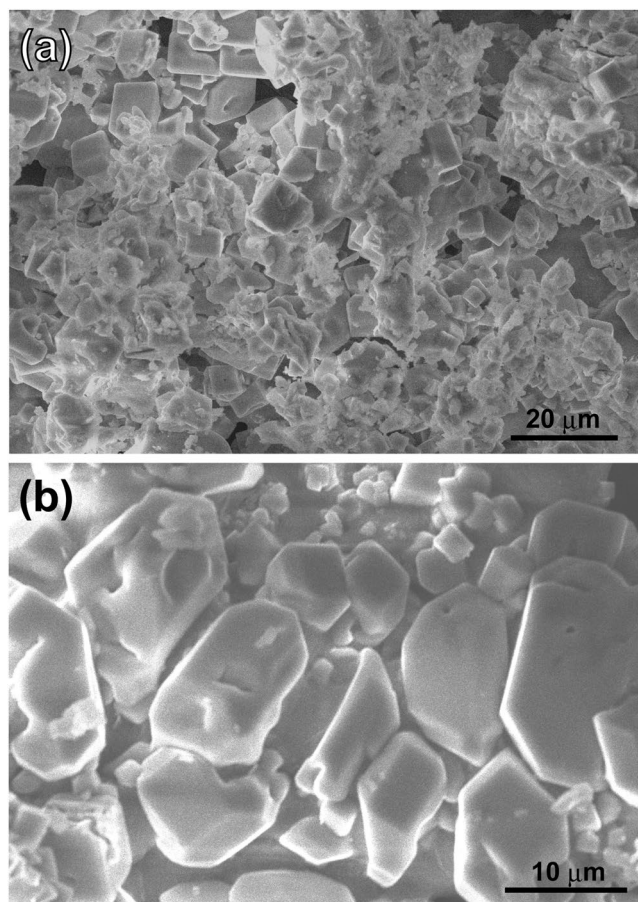


**Figure 2.** (a,b) SEM images for the optimal sample at low and high magnifications.

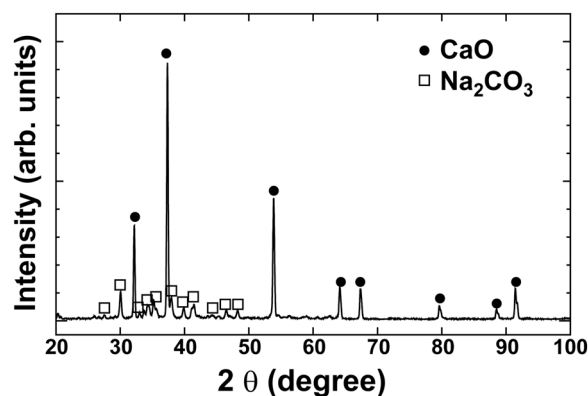


**Figure 3.** X-ray diffraction profile for the optimal sample, showing two phases of CaO (JCPDF#37-1497) and Na<sub>2</sub>CO<sub>3</sub> (#37-0451).

further characterised the microstructure of the optimised sample. Notably, the product without Ca obtained by the PC method shows poor performance (0.8~1%).

Figure 2 shows the SEM images at low and high magnifications. The particle sizes varied from 10 to 20 microns, and the nominal composition was Ca<sub>13.7</sub>Na<sub>13.3</sub>C<sub>8.4</sub>O<sub>64.4</sub>Cl<sub>0.2</sub> (at.%) as determined by SEM-EDS analysis. EDS analysis results for the samples with different NaCl/Ca ratios are summarised in Table S1. The doping of Cl was also confirmed, and the Brunauer–Emmett–Teller (BET) surface area was calculated to be 4.6 m<sup>2</sup>/g (Fig. S1). Unexpectedly, the X-ray diffraction profile shows that the optimal sample contains two phases, CaO (JCPDF#37-1497) and Na<sub>2</sub>CO<sub>3</sub> (#37-0451), as shown in Fig. 3. We also recorded the X-ray diffraction profiles (XRD) patterns for samples with different NaCl/Ca ratios (Fig. S2 in Supporting Information). The XRD patterns indicated that all the samples contain two phases, CaO and Na<sub>2</sub>CO<sub>3</sub>. Moreover, the energy-dispersive X-ray spectroscopy (EDS)

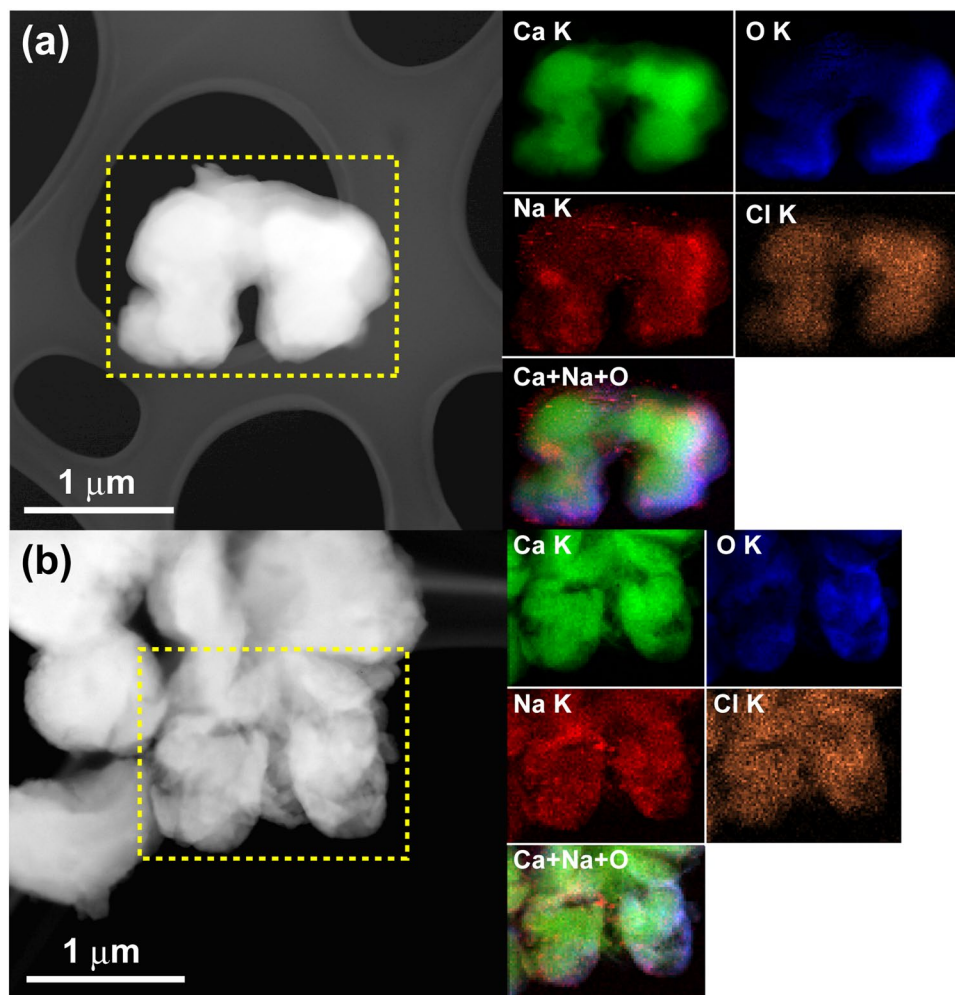


**Figure 4.** (a,b) STEM image and EDS chemical maps of the selected area, showing the distributions of Ca (green), Na (red), O (blue), and Cl (orange) and the mixture of Ca + Na + O.

mapping analysis and scanning transmission electron microscopy (STEM) data, as shown in Fig. 4, clearly displays the uniform coverage by Na of  $\text{Na}_2\text{CO}_3$  over CaO fine particles. The melting temperature of  $\text{Na}_2\text{CO}_3$  was  $851^\circ\text{C}$ , and the optimal temperature ( $950^\circ\text{C}$ ) is far above that. Therefore,  $\text{Na}_2\text{CO}_3$  works as a molten salt catalyst, and the melting behaviour observed was very stark from the morphology change whenever we checked the sample after the catalytic tests, as shown in Fig. S3. The TGA results also confirmed the melting state of  $\text{Na}_2\text{CO}_3$  at  $950^\circ\text{C}$ , as shown in Fig. S4.

We performed *in situ* Fourier transform infrared (FTIR) experiments to clarify the mechanism of hydrocarbon synthesis, at the reaction temperature shown in Fig. 5(a), and we confirmed the existence of carbonyl ( $\text{M}=\text{C}=\text{O}$ ) and methane radical groups ( $-\text{CH}_3$ ). The suggestive mechanism has been outlined in Fig. 5(b). Because  $\text{Na}_2\text{CO}_3$  can decompose to  $\text{Na}_2\text{O} + \text{CO}_2$  above the melting temperature<sup>17</sup>,  $\text{Na}_2\text{O}$  on the surface could convert  $\text{CH}_4$  to  $\text{CH}_3$  radicals with CaO<sup>18,19</sup> with the assistance of Cl dopants efficiently. Accordingly, two or more  $\text{CH}_3$  radicals were coupled towards the production of  $\text{C}_{2,3}$  hydrocarbons, as has been reported previously<sup>11</sup>. Further investigations are needed to provide a clearer mechanism.

We checked the durability of the optimal catalyst, as shown in Fig. 6(a) and the  $\text{C}_{2,3}$  yield gradually decreased over time. STEM imaging with EDS mapping after the catalytic test was employed as shown in Fig. 6(b) and it showed a reduction in the Na coverage and reduced detection of Cl over CaO particles, thus demonstrating the major reason for degradation of hydrocarbon production. The XRD patterns and X-ray photoelectron spectroscopy (XPS) profiles after the experiment also showed the signal reduction of Na and Cl (Figs S5–S7). Regarding the XPS profiles, by comparison with the Ca profile in the sample with (Fig. S6a) and without 20% NaCl (Fig. S6c), two kinds of peaks of Ca  $2p_{3/2}$  can be observed as shown in Fig. S6c. Their binding energies are about 345.0 eV and 346.5 eV, which correspond to Ca metallic bonding and CaO insulating ones, respectively<sup>20</sup>. Moreover, the spitting of Cl  $2p_{3/2}$  as shown in Fig. S6b demonstrates that Ca-Cl and Na-Cl are in the sample with NaCl. These results indicate that NaCl in the CaO- $\text{Na}_2\text{CO}_3$  could contribute to the refusion of CaO and  $\text{Na}_2\text{CO}_3$ . After long-term testing of our optimal sample, a new peak located at 347.0 eV appeared as shown in Fig. S7c,

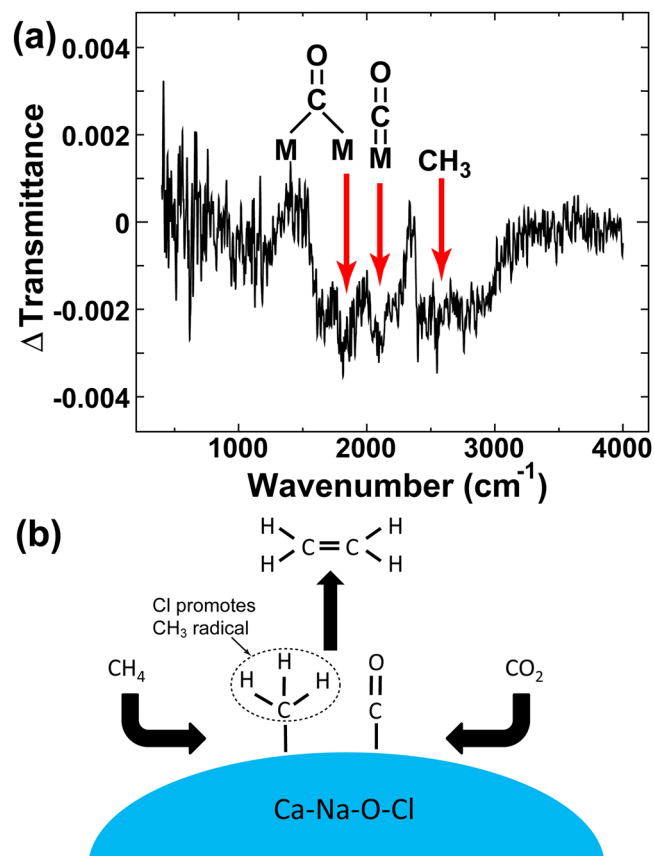


**Figure 5.** (a) FTIR difference spectrum for the optimal sample, which was obtained by subtracting the spectrum obtained for 25 min after leaching at 900 °C from that obtained for 30 min. (b) Proposed mechanism for the formation of hydrocarbons over the Ca–Na–O–Cl catalyst.

which corresponds to  $\text{CaCO}_3$ . It indicates that some  $\text{CaO}$  turned to  $\text{CaCO}_3$  after long-term testing. It should be noted that the content of Cl goes to zero after long-term tests.

Since mass reduction via evaporation is a major concern of alkali molten catalysts in general<sup>21</sup>, this issue must be given attention to further improve our results. Suppressing mass reduction is thus a topic of future research underway in our group as well as the design of other suitable reactor designs such as a bubbling system<sup>22</sup> and/or increasing the pressure of the gas atmosphere to gain more hydrocarbons.

## Conclusion

In summary, we have fabricated a complex  $\text{CaO}$ -based oxide by the PC method, in which we achieved uniform  $\text{Na}_2\text{CO}_3$  covered with  $\text{CaO}$  fine particles with Cl dopants. The optimal composition gave the highest  $\text{C}_{2,3}$  yield of 6.6% at 950 °C via  $\text{CO}_2$ -OCM.  $\text{Na}_2\text{CO}_3$  works as a molten salt catalyst at the reaction temperature, and the suppression of mass reduction is an issue requiring further studies for improvement. Because the proposed catalysts are inexpensive and truly earth abundant, our method could contribute to achieving higher yields of hydrocarbons in the future.

## Methods

**Sample preparation.** The following procedure is based on a modified polymerised complex (PC) method<sup>23</sup> to achieve the optimum composition in this study. The molar ratio of each chemical can be varied, as described in the results. Calcium citrate ( $\text{Ca}_3(\text{C}_6\text{H}_5\text{O}_7)_2 \cdot 4\text{H}_2\text{O}$ , Wako, 97.0%), trisodium citrate ( $\text{C}_6\text{H}_5\text{Na}_3\text{O}_7$ , Wako, 99.0%), and L-aspartic acid ( $\text{C}_4\text{H}_7\text{NO}_4$ , Wako, 99.0%) were dissolved in deionised water at a molar ratio of 1:1:9. After ultrasonic treatment for 5 min, 69% (wt.%) nitric acid ( $\text{HNO}_3$ , Wako) was added dropwise until all of the calcium citrate powder in the solution dissolved. Next, sodium chloride ( $\text{NaCl}$ , Wako, 99.5%) was dissolved in a solution with a 60% molar content of calcium citrate, i.e.,  $\text{NaCl}:\text{Ca} = 0.2:1$  (by mol). After drying at 120 °C for 12 h in the oven, a pale-yellow precursor was formed. A final annealing process was conducted in an alumina combustion boat at 700 °C for 2 h in air. After the heat treatment, a white powder was obtained after cooling naturally to room temperature.

For comparison with the PC method, the following simple mixing procedure for obtaining the optimal composition was employed: 0.1 mol calcium oxide ( $\text{CaO}$ , Wako, 99.9%) was dispersed into 100 mL of deionised water and then 0.1 mol sodium hydroxide ( $\text{NaOH}$ , Wako, 97.0%) and 0.02 mol sodium chloride ( $\text{NaCl}$ , Wako, 99.5%) were added to the solution. After ultrasonic treatment for 5 min, the turbid solution was dried at 120 °C for 12 h



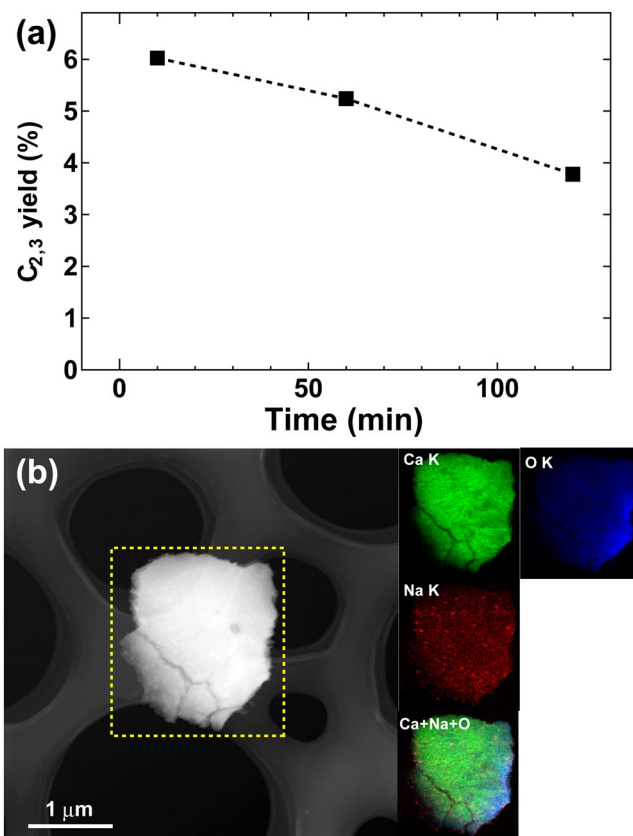


**Figure 6.** (a) Durability test for the optimal sample. (b) STEM image and EDS chemical maps of the spent sample, showing the distributions of Ca (green), Na (red), and O (blue) and the mixture of Ca + Na + O. Cl elements were not detected sufficiently for visualisation.

in the oven. The precursor was transferred to an alumina combustion boat and a final annealing process was conducted at 700 °C for 2 h in air. After the heat treatment, white powders were obtained.

**Characterisation.** Microstructures of the obtained catalysts were characterised by transmission electron microscopy (TEM, JEM-2100F, JEOL, equipped with aberration correctors, for the image- and probe-forming lens systems, CEOS GmbH) and energy-dispersive X-ray spectrometry (EDS, JED-2300T, JEOL). High-resolution TEM (HRTEM) and scanning TEM (STEM) observations were conducted at an accelerating voltage of 200 kV with the Cs correctors. The samples were transferred onto a Cu grid without the use of a uniform carbon support film<sup>24</sup>. The microstructures of the samples were also characterised by using a field-emission scanning electron microscopy (SEM; JEOL JIB-4600F, 15 kV) system equipped with an X-ray energy-dispersive spectrometry apparatus. X-ray diffraction profiles (XRD) were obtained by using a Rigaku SmartLab X-ray diffractometer with Cu K $\alpha$  radiation at 30 kV<sup>24</sup>. The samples were analysed by thermogravimetry-differential thermal analysis (TG-DTA, NETZCH, STA 2500) under nitrogen. The temperature was increased at the rate of 20 K/min. The chemical state of the samples was measured by X-ray photoelectron spectroscopy (XPS; AXIS ultra DLD, Shimadzu) with a monochromated AlK $\alpha$  radiation source.

**Catalytic experiments.** The desired sample (100 mg) was loaded into a 4-mm-diameter quartz tube and tested by using a continuous-flow fixed-bed microreactor under atmospheric pressure. The quantities of CH<sub>4</sub>, CO, H<sub>2</sub>, CO<sub>2</sub>, C<sub>2</sub>H<sub>2</sub>, C<sub>2</sub>H<sub>4</sub>, C<sub>2</sub>H<sub>6</sub>, C<sub>3</sub>H<sub>6</sub>, and C<sub>3</sub>H<sub>8</sub> were monitored and evaluated by using an on-line gas analyser (BELMass, MicrotracBEL) and a gas chromatograph (GC-2014 and Trasera, Shimadzu, Japan) equipped with a thermal conductivity detector, flame ionisation detector, and barrier ionisation detector<sup>24</sup>. The reactant gas containing 1 vol.% CH<sub>4</sub>, 1 vol.% CO<sub>2</sub>, and He to compensate was introduced into the reactor at a space velocity (SV) of 10 cm<sup>3</sup> min<sup>-1</sup> (W/F = 0.6 g s cm<sup>-3</sup>). The optimum reaction temperature to obtain the maximum C<sub>2,3</sub> yield was 950 °C and was instrumentally the upper limit. The calculations were conducted by using the following formulae<sup>25</sup>:

$$\text{CH}_4 \text{ conversion [\%]} = \frac{[\text{CH}_4]_{\text{in}} - [\text{CH}_4]_{\text{out}}}{[\text{CH}_4]_{\text{in}}} \times 100$$

$$C_{2,3}\text{yield (carbon base)}[\%] = \frac{2[C_2H_2]_{\text{out}} + 2[C_2H_4]_{\text{out}} + 2[C_2H_6]_{\text{out}} + 3[C_3H_6]_{\text{out}} + 3[C_3H_8]_{\text{out}}}{[CH_4]_{\text{in}}} \times 100$$

Therefore, selectivity of ethane, as an example (carbon base) [%]

$$= \frac{2[C_2H_6]_{\text{out}}}{2[C_2H_2]_{\text{out}} + 2[C_2H_4]_{\text{out}} + 2[C_2H_6]_{\text{out}} + 3[C_3H_6]_{\text{out}} + 3[C_3H_8]_{\text{out}}} \times 100$$

where  $[\dots]_{\text{in}}$  and  $[\dots]_{\text{out}}$  represent the gas concentrations in the feed gas and effluent gas, respectively.

**Surface area measurements and analysis.** The Brunauer–Emmett–Teller (BET) surface areas of the samples were measured at 77 K by using a BELSORP-MAX II (MicrotracBEL Japan, Inc.). Each sample was heated at 120 °C under vacuum for 24 h prior to measurement, and the mass of each sample was measured by using a balance<sup>24</sup>.

FTIR spectra of the catalyst surfaces were measured at the operating temperature by using a JASCO 6100 FTIR system equipped with a heat chamber (ST-Japan). Each sample (5 mg) was loaded onto the sample stage, and the reactant gas containing 1 vol.% CH<sub>4</sub>, 1 vol.% CO<sub>2</sub>, and Ar to compensate was introduced into the environmental cell at a rate of 10 cm<sup>3</sup> min<sup>-1</sup><sup>24</sup>.

### Data availability

The datasets generated during and/or analysed during the current study are available from the corresponding author on reasonable request.

Received: 26 March 2019; Accepted: 7 October 2019;

Published online: 29 October 2019

### References

- Muraza, O. & Galadima, A. A review on coke management during dry reforming of methane. *Int. J. Energy Res.* **39**, 1196–1216 (2015).
- Lavoie, J. M. Review on dry reforming of methane, a potentially more environmentally-friendly approach to the increasing natural gas exploitation. *Front. Chem.* **2**, 81 (2014).
- Cai, X. & Hu, Y. H. Advances in catalytic conversion of methane and carbon dioxide to highly valuable products. *Energy Sci. Eng.* **7**, 4–29 (2019).
- Asami, K., Fujita, T., Kusakabe, K. I., Nishiyama, Y. & Ohtsuka, Y. Conversion of methane with carbon dioxide into C2 hydrocarbons over metal oxides. *Appl. Catal. A Gen.* **126**, 245–255 (1995).
- Ito, T., Wang, J., Lin, C. H. & Lunsford, J. H. Oxidative dimerization of methane over a lithium-promoted magnesium oxide catalyst. *J. Am. Chem. Soc.* **107**, 5062–5068 (1985).
- Ross, J. R. H., van Keulen, A. N. J., Hegarty, M. E. S. & Seshan, K. The catalytic conversion of natural gas to useful products. *Catal. Today* **30**, 193–199 (1996).
- Olivos-Suarez, A. I. *et al.* Strategies for the direct catalytic valorization of methane using heterogeneous catalysis: Challenges and opportunities. *ACS Catal.* **6**, 2965–2981 (2016).
- Arndt, S. *et al.* A critical assessment of Li/MgO-based catalysts for the oxidative coupling of methane. *Catal. Rev.* **53**, 424–514 (2011).
- Asami, K. *et al.* Formation of ethane and ethylene by the reaction of methane and carbon dioxide over unsupported metal oxides. *Stud. Surf. Sci. Catal.* **107**, 279–283 (1997).
- Wang, Y., Takahashi, Y. & Ohtsuka, Y. Carbon dioxide as oxidant for the conversion of methane to ethane and ethylene using modified CeO<sub>2</sub> catalysts. *J. Catal.* **186**, 160–168 (1999).
- Wang, Y., Takahashi, Y. & Ohtsuka, Y. Carbon dioxide-induced selective conversion of methane to C2 hydrocarbons on CeO<sub>2</sub> modified with CaO. *Appl. Catal. A Gen.* **172**, L203–L206 (1998).
- Kakihana, M. Invited review “sol-gel” preparation of high temperature superconducting oxides. *J. Sol-Gel Sci. Technol.* **6**, 7–55 (1996).
- Kakihana, M. & Yoshimura, M. Synthesis and characteristics of complex multicomponent oxides prepared by polymer complex method. *Bull. Chem. Soc. Jpn.* **72**, 1427–1443 (1999).
- Michelsen, H. A. The reaction of Cl with CH<sub>4</sub>: A connection between kinetics and dynamics. *Acc. Chem. Res.* **34**, 331–337 (2001).
- Niggli, P. Untersuchungen an Karbonat- und -chloridschmelzen. *Z. Anorg. Allg. Chem.* **106**, 126–142 (1919).
- Mitchell, R. H. & Kjarsgaard, B. A. Experimental studies of the system Na<sub>2</sub>Ca(CO<sub>3</sub>)<sub>2</sub>–NaCl–KCl at 0.1 GPa: implications for the differentiation and low-temperature crystallization of natrocarbonatite. *Can. Mineral.* **46**, 971–980 (2008).
- Motzfeldt, K. The thermal decomposition of sodium carbonate by the effusion method. *J. Phys. Chem.* **59**, 139–147 (1955).
- Spinicci, R. Oxidative coupling of methane as studied by temperature programmed reaction and transient response methods. *Catal. Today* **4**, 311–322 (1989).
- Wong, N. B., Tin, K. C., Lau, K., Qiu, X. Q. & Zhu, Q. M. Oxidative coupling of methane over alkali metal oxide promoted La<sub>2</sub>O<sub>3</sub>/BaCO<sub>3</sub> catalysts. *J. Chem. Technol. Biotechnol.* **65**, 351–354 (1996).
- Itti, R. *et al.* Photoelectron spectroscopic study of (Y<sub>1-x</sub>Ca<sub>x</sub>)Ba<sub>2</sub>Cu<sub>3</sub>O<sub>7-y</sub>: Observation of the Fermi-edge-like structure at room temperature. *Phys. Rev. B* **41**, 9559–9562 (1990).
- Kenney, C. N. Molten salt catalysis of gas reactions. *Catal. Rev.* **11**, 197–224 (1975).
- Upham, D. C. *et al.* Catalytic molten metals for the direct conversion of methane to hydrogen and separable carbon. *Science* **358**, 917–921 (2017).
- Sugahara, K., Kamata, K., Muratsugu, S. & Hara, M. Amino acid-aided synthesis of a hexagonal SrMnO<sub>3</sub> nanoperovskite catalyst for aerobic oxidation. *ACS Omega* **2**, 1608–1616 (2017).
- Fujita, T. *et al.* Nanoporous nickel composite catalyst for the dry reforming of methane. *ACS Omega* **3**, 16651–16657 (2018).
- Sato, A. *et al.* Ambient-temperature oxidative coupling of methane in an electric field by a cerium phosphate nanorod catalyst. *Chem. Comm.* **55**, 4019–4022 (2019).

## Acknowledgements

This study was mainly supported by the JST-CREST program ‘Innovative catalysts and creation technologies for the utilisation of diverse natural carbon resources’ (grant no. JPMJCR15P1) and was partially supported by KAKENHI (grant No. JP16H02293). We also acknowledge support from Prof. Mingwei Chen for allowing the use of TEM services at Tohoku University. The authors thank Ms. Kazuyo Omura of the Institute for Material Research at Tohoku University for carrying out the XPS measurements.

## Author contributions

Y.-Z.Z. fabricated the samples, Y.C. analysed the samples by XRD, and A.Y. and M.M. performed the FTIR experiments. T.F. designed the sample compositions, characterised the samples, and performed catalytic tests. X.P. assisted with the catalytic tests. T.F. wrote the manuscript, and all authors reviewed the manuscript. T.F., M.M. and H.A. supervised the project.

## Competing interests

The authors declare no competing interests.

## Additional information

**Supplementary information** is available for this paper at <https://doi.org/10.1038/s41598-019-51817-2>.

**Correspondence** and requests for materials should be addressed to T.F.

**Reprints and permissions information** is available at [www.nature.com/reprints](http://www.nature.com/reprints).

**Publisher’s note** Springer Nature remains neutral with regard to jurisdictional claims in published maps and institutional affiliations.



**Open Access** This article is licensed under a Creative Commons Attribution 4.0 International License, which permits use, sharing, adaptation, distribution and reproduction in any medium or format, as long as you give appropriate credit to the original author(s) and the source, provide a link to the Creative Commons license, and indicate if changes were made. The images or other third party material in this article are included in the article’s Creative Commons license, unless indicated otherwise in a credit line to the material. If material is not included in the article’s Creative Commons license and your intended use is not permitted by statutory regulation or exceeds the permitted use, you will need to obtain permission directly from the copyright holder. To view a copy of this license, visit <http://creativecommons.org/licenses/by/4.0/>.

© The Author(s) 2019